

Indirect Signatures of Gravitino Dark Matter

Alejandro Ibarra

*DESY, Theory Group, Notkestrasse 85, D-22603 Hamburg, Germany
Physik Department T30, Technische Universität München,
James-Franck-Strasse, 85748 Garching, Germany*

Abstract.

Supersymmetric models provide very interesting scenarios to account for the dark matter of the Universe. In this talk we discuss scenarios with gravitino dark matter in R -parity breaking vacua, which not only reproduce very naturally the observed dark matter relic density, but also lead to a thermal history of the Universe consistent with the observed abundances of primordial elements and the observed matter-antimatter asymmetry. In this class of scenarios the dark matter gravitinos are no longer stable, but decay with very long lifetimes into Standard Model particles, thus opening the possibility of their indirect detection. We have computed the expected contribution from gravitino decay to the primary cosmic rays and we have found that a gravitino with a mass of $m_{3/2} \sim 150$ GeV and a lifetime of $\tau_{3/2} \sim 10^{26}$ s could simultaneously explain the EGRET anomaly in the extragalactic gamma-ray background and the HEAT excess in the positron fraction.

Keywords: Dark matter, Supersymmetric models, Cosmic rays

PACS: 95.35.+d, 12.60.Jv, 98.70.Sa

INTRODUCTION

A series of observations have provided in recent years compelling evidences for the existence of dark matter in the Universe [1]. These observations have revealed that the dark matter particle has to be weakly interacting with the ordinary matter, long lived and slow moving (“cold”). Among the most interesting candidates proposed stands the gravitino [2] which is abundantly produced by thermal scatterings in the very early Universe. If the gravitino is the lightest supersymmetric particle (LSP), a fraction of their initial population will survive until today with a relic density which is calculable in terms of very few parameters, the result being [3]

$$\Omega_{3/2} h^2 \simeq 0.27 \left(\frac{T_R}{10^{10} \text{ GeV}} \right) \left(\frac{100 \text{ GeV}}{m_{3/2}} \right) \left(\frac{m_{\tilde{g}}}{1 \text{ TeV}} \right)^2, \quad (1)$$

where T_R is the reheating temperature of the Universe, $m_{3/2}$ is the gravitino mass and $m_{\tilde{g}}$ is the gluino mass. In predicting the relic abundance of gravitinos, the main uncertainty arises from our ignorance of the thermal history of the Universe before Big Bang nucleosynthesis (BBN) and in particular of the reheating temperature after inflation. However, we have strong indications that the Universe was very hot after inflation. Namely, the discovery of neutrino masses provided strong support to leptogenesis as the explanation for the observed baryon asymmetry of the Universe [4]. This mechanism can reproduce the observed baryon asymmetry very naturally if the reheating temperature of the Universe was above 10^9 GeV [5]. Therefore, the abundance of gravitinos can reproduce the dark matter relic density inferred by

WMAP for the Λ CDM model, $\Omega_{\text{CDM}} h^2 \simeq 0.1$ [6], for natural values of the input parameters in Eq. (1).

Being capable of reproducing the correct relic density is a necessary requirement for any dark matter candidate, but not the only one. Namely, the physical model accounting for the dark matter should not spoil the successful predictions of the standard cosmology. However, in scenarios with gravitino dark matter, when R -parity is conserved, the next-to-LSP (NLSP) is typically present during or after Big Bang nucleosynthesis, jeopardizing the successful predictions of the standard nucleosynthesis scenario. This is in fact the case for the most likely candidates for the NLSP: the lightest neutralino and the right-handed stau. More precisely, when the NLSP is the neutralino, the hadrons produced in the neutralino decays typically dissociate the primordial elements [7], yielding abundances in conflict with observations. On the other hand, when the NLSP is a charged particle, X^- , the formation of the bound state (${}^4\text{He}X^-$) catalyzes the production of ${}^6\text{Li}$ [8] leading to an overproduction of ${}^6\text{Li}$ by a factor 300 – 600 [9].

Different solutions have been proposed to this problem. For instance, in some specific supersymmetric models the NLSP can be a sneutrino [10] or a stop [11], whose late decays do not substantially affect the predictions of Big Bang nucleosynthesis. Other solutions are to assume a large left-right mixing of the stau mass eigenstates [12] or to assume some amount of entropy production after NLSP decoupling, which dilutes the NLSP abundance [13]. Our proposed solution consists in introducing a small amount of R -parity violation, so that the NLSP decays into two Standard Model particles before

the onset of Big Bang nucleosynthesis, thus avoiding the BBN constraints altogether [14].

GRAVITINO DECAY

When R -parity is not exactly conserved, the gravitino LSP is no longer stable. Nevertheless, the gravitino decay rate is doubly suppressed by the Planck mass and by the small R -parity violation [15]. Therefore, for the range of R -parity violating couplings favored by cosmology, the gravitino lifetime ranges between 10^{23} and 10^{37} s for $m_{3/2} = 100$ GeV, which exceeds the age of the Universe by many orders of magnitude. Hence, even though the gravitino is not absolutely stable, it is stable enough to constitute a viable candidate for the dark matter of the Universe, while preserving the attractive features of the standard Big Bang nucleosynthesis scenario and thermal leptogenesis.

Interestingly, gravitinos could be decaying at a rate sufficiently large to allow the detection of the decay products in experiments, thus opening the possibility of the indirect detection of the elusive gravitino dark matter.

In this talk we will discuss the possibility that gravitinos are heavier than the gauge bosons. If this is the case, gravitinos decay mainly into three different channels [16, 17, 18]: $\psi_{3/2} \rightarrow \gamma v$, $W^\pm \ell^\mp$, $Z^0 v$. The fragmentation of the W^\pm and the Z^0 eventually produces a flux of stable particles, which we have simulated with the event generator PYTHIA 6.4 [19]. On the other hand, the branching ratios of the different decay channels are also calculable in the framework of supergravity with broken R -parity, yielding a result that depends mainly on the gravitino mass (under the popular assumption of gaugino mass unification at the Grand Unification scale).

Dark matter gravitinos populate the halo with a distribution that follows a density profile $\rho(\vec{r})$, where \vec{r} denotes the position with respect to the center of the Galaxy. We will adopt for our numerical analysis the Navarro-Frenk-White density profile [20]:

$$\rho(r) = \frac{\rho_0}{(r/r_c)[1 + (r/r_c)]^2}, \quad (2)$$

with $\rho_0 \simeq 0.26 \text{ GeV}/\text{cm}^3$ and $r_c \simeq 20$ kpc, although our conclusions are not very sensitive to the choice of the density profile. Gravitinos at \vec{r} eventually decay with lifetime $\tau_{3/2}$ producing photons, positrons, antiprotons and neutrinos at a rate per unit energy and unit volume given by

$$Q_x(E, \vec{r}) = \frac{\rho(\vec{r})}{m_{3/2} \tau_{3/2}} \frac{dN_x}{dE}, \quad (3)$$

where $x = \gamma, e^+, \bar{p}, \nu$ and dN_x/dE is the energy spectrum of the particle x produced in the decay. Remarkably,

the source function depends essentially on two unknown parameters, namely the gravitino mass and the gravitino lifetime, yielding a fairly predictive scenario.

We will present in this talk the results for the gamma-ray flux [16] and for the positron and antiproton fluxes [17]. The results for the neutrino flux will be presented elsewhere [21]. The flux at Earth of the different particle species are constrained by a series of experiments. EGRET measured gamma-rays in the energy range between 30 MeV to 100 GeV. After subtracting the galactic foreground emission, the residual flux was found to be roughly isotropic and thus attributed to extragalactic sources. An improved analysis of the galactic foreground by Strong *et al.* [22], optimized in order to reproduce the galactic emission, shows a power law behavior between 50 MeV–2 GeV, but a clear excess between 2–10 GeV, roughly the same energy range where one would expect a signal from gravitino decay. On the other hand, the flux of positrons has been measured by a series of experiments, in particular by HEAT [23]. Although the measurements still suffer from large uncertainties, it is intriguing that all the experiments seem to point to an excess of positrons at energies larger than 7 GeV, which is again the energy range where a contribution to the flux from gravitino decay is expected. Lastly, the measurements of the antiproton flux by BESS [24] and other experiments do not show any deviation from the predictions by conventional astrophysical models of spallation of cosmic rays on the Milky Way disk. Future experiments such as the FGST (formerly GLAST) [25], measuring the gamma-ray flux, and PAMELA [26], measuring antimatter fluxes, will provide in the near future very precise measurements of the spectra of cosmic rays which will constitute decisive tests of the decaying dark matter scenario.

GAMMA-RAY FLUX

The gamma-ray flux from gravitino decay has two components. The decay of gravitinos at cosmological distances will be detected at Earth as a perfectly isotropic diffuse gamma-ray background with a red-shifted energy spectrum. A second source of gamma-rays is the decay of gravitinos in the Milky Way halo. For typical halo models, we find that the halo component dominates over the cosmological one [14, 27], yielding a slightly anisotropic gamma-ray flux.

The different contributions to the total gamma-ray flux from gravitino decay are shown in Fig. 1 for a mass of $m_{3/2} \sim 150$ GeV and a lifetime of $\tau_{3/2} \sim 1.3 \times 10^{26}$ s [16]. To compare our results with the EGRET data [22], also shown in the figure, we have averaged the halo signal over the whole sky excluding a band of

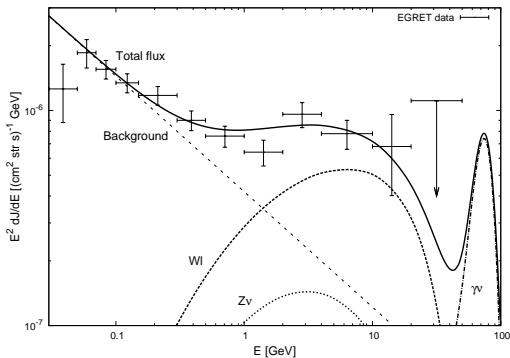


FIGURE 1. Contributions to the total gamma-ray flux for $m_{3/2} = 150\text{ GeV}$ and $\tau_{3/2} \simeq 1.3 \times 10^{26}\text{ s}$ compared to the EGRET data. In dotted lines we show the photon flux from the fragmentation of the Z boson, in dashed lines from the fragmentation of the W boson, and in dot-dashed lines from the two body decay $\psi_{3/2} \rightarrow \gamma\nu$. The background is shown as a long dashed line, while the total flux received is shown as a thick solid line.

$\pm 10^\circ$ around the Galactic disk, and we have used an energy resolution of 15%, as quoted by the EGRET collaboration in this energy range. The energy resolution of the detector is particularly important to determine the width and the height of the monochromatic line stemming from the two body decay $\psi_{3/2} \rightarrow \gamma\nu$. The three contributions are dominated by the halo component, the extragalactic component being smaller by a factor of 2–3. Finally, we have adopted an energy spectrum for the extragalactic background described by the power law $\left[\frac{d\Phi_\nu}{dE}\right]_{bg} = 4 \times 10^{-7} \left(\frac{E}{\text{GeV}}\right)^{-2.5} (\text{cm}^2\text{str s GeV})^{-1}$, in order to provide a good agreement of the total flux received with the data.

The predicted energy spectrum shows two qualitatively different features. At energies between 1–10 GeV, we expect a continuous spectrum of photons coming from the fragmentation of the gauge bosons. As a result, the predicted spectrum shows a departure from the power law in this energy range that might be part of the apparent excess inferred from the EGRET data by Strong *et al.* [22]. In addition to the continuous component, the energy spectrum shows a relatively intense monochromatic line at higher energies arising from the decay channel $\psi_{3/2} \rightarrow \gamma\nu$.

Even though the gamma-ray flux from gravitino decay is expected to be anisotropic, we find that with these parameters the flux resembles an isotropic extragalactic flux in EGRET. Namely, in the energy range 0.1–10 GeV, the anisotropy between the Inner Galaxy region ($|b| > 10^\circ, 270^\circ \leq l \leq 90^\circ$) and the Outer Galaxy region ($|b| > 10^\circ, 90^\circ \leq l \leq 270^\circ$) is just a 6%, well compatible with the EGRET data [22].

ANTIMATTER FLUX

Antimatter propagation in the Milky Way is commonly described by a stationary two-zone diffusion model with cylindrical boundary conditions [28]. Neglecting re-acceleration effects and non-annihilating interactions of antimatter in the Galactic disk, the propagation can be described by only a few parameters, which can be determined from the flux measurements of other cosmic ray species, mainly from the Boron to Carbon (B/C) ratio [29].

The solution of the transport equation at the Solar System can be formally expressed by the convolution

$$f(T) = \frac{1}{m_{3/2}\tau_{3/2}} \int_0^{T_{\max}} dT' G(T, T') \frac{dN(T')}{dT'}, \quad (4)$$

where T is the kinetic energy and $T_{\max} = m_{3/2}$ for the case of the positrons while $T_{\max} = m_{3/2} - m_p$ for the antiprotons. The solution is thus factorized into two parts. The first part, given by the Green's function $G(T, T')$, encodes all of the information about the astrophysics (such as the details of the halo profile and the complicated propagation of antiparticles in the Galaxy) and is universal for any decaying dark matter candidate. The remaining part depends exclusively on the nature and properties of the decaying dark matter candidate, namely the mass, the lifetime and the energy spectrum of antiparticles produced in the decay. Finally, the flux of primary antiparticles at the Solar System from dark matter decay is given by:

$$\Phi^{\text{prim}}(T) = \frac{v}{4\pi} f(T), \quad (5)$$

where v is the velocity of the antimatter particle.

Clearly, if gravitino decay is the explanation for the extragalactic EGRET anomaly, our predicted positron and antiproton fluxes should not exceed the measured ones. In the scenario we are considering the gravitino mass and lifetime are constrained by requiring a qualitatively good agreement of the predicted extragalactic gamma-ray flux with the EGRET data: $m_{3/2} = 150\text{ GeV}$ and $\tau_{3/2} = 1.3 \times 10^{26}\text{ s}$ [16]. On the other hand, the energy spectrum of antiparticles, dN/dT , is determined by the physics of fragmentation. Therefore, the main uncertainty in the computation of the antimatter fluxes stems from the determination of the Green's function, *i.e.* from the uncertainties in the propagation parameters and the halo profile. We have found in our analysis that the uncertainties in the precise shape of the halo profile are not crucial for the determination of the primary antimatter fluxes. On the other hand, the uncertainties in the propagation parameters can substantially change the predictions for the antimatter fluxes, even by two orders of magnitude for the antiproton flux.

Positrons and antiprotons have different properties and their respective transport equations can be approximated

TABLE 1. Coefficients of the interpolating function Eq. (6) for the positron Green’s function, assuming a NFW halo profile and for the M2, MED and M1 propagation models defined in [30].

model	a	b
M2	-0.9716	-10.012
MED	-1.0203	-1.4493
M1	-0.9809	-1.1456

by different limits of the transport equation. Let us discuss each case separately.

Positron flux

In the case of positron propagation, galactic convection and annihilations in the disk can be neglected in the transport equation. We have solved the transport equation and computed the Green’s function for three propagation models, denoted as M2, MED and M1, which are consistent with the B/C ratio and which yield, respectively, the minimum, median and maximal positron flux [30]. The Green’s function from dark matter decay can be well approximated by the following interpolating function [17]:

$$G_{e^+}(T, T') \simeq \frac{10^{16}}{T^2} e^{a+b(T^{\delta-1}-T'^{\delta-1})} \theta(T'-T) \text{cm}^{-3} \text{s}, \quad (6)$$

where T and T' are expressed in units of GeV. The coefficients a and b for each propagation model can be found in Table 1 for the NFW profile. This approximation works better than a 15-20% over the whole range of energies. It should be stressed that this parametrization of the Green’s function is valid for *any* decaying dark matter particle, not just for the gravitino.

With the previous parametrization of the Green’s function, it is straightforward to compute the interstellar positron flux using Eqs. (4) and Eq. (5). The total positron flux received at Earth receives, in addition to the primary flux from gravitino decay, a secondary component originating in the collision of primary protons and other nuclei on the interstellar medium, which constitutes the background to our signal.

To compare our predicted flux with the observations we choose to show the positron fraction, defined as the total positron flux divided by the total electron plus positron fluxes:

$$\text{PF}(T) = \frac{\Phi_{e^+}^{\text{prim}}(T) + \Phi_{e^+}^{\text{sec}}(T)}{\Phi_{e^+}^{\text{prim}}(T) + \Phi_{e^+}^{\text{sec}}(T) + k \Phi_{e^-}^{\text{prim}}(T) + \Phi_{e^-}^{\text{sec}}(T)}, \quad (7)$$

where following [31, 32] we have left the normalization of the primary electron flux, k , as a free parameter to be fitted in order to match the observations of the positron

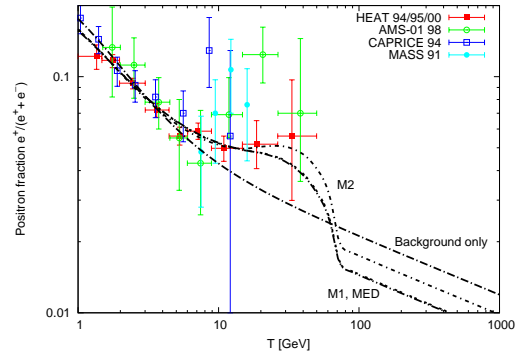


FIGURE 2. Positron fraction from the decay of gravitinos for a NFW halo profile and the M2, MED and M1 propagation models. Gravitino parameters are as in Fig. 1. We also show for comparison the contribution to the positron fraction from spallation of cosmic rays on the Galactic disk, which constitutes the background to our signal.

fraction. For the flux of secondary positrons, and the primary and secondary electrons we used the parametrizations obtained in [31] from detailed computer simulations of cosmic ray propagation [33].

We show in Fig. 2 the positron fraction for different diffusion models in the case of the NFW profile when $m_{3/2} \simeq 150 \text{ GeV}$ and $\tau_{3/2} \simeq 1.3 \times 10^{26} \text{ s}$. Interestingly, we find that gravitino parameters which predict a departure from a simple power law in the extragalactic gamma-ray spectrum at energies above 2 GeV (as observed by EGRET), *inevitably* predict a bump in the positron fraction at energies above 7 GeV (as observed by HEAT) [17]¹. Furthermore, the presence of this feature is not very sensitive to the many astrophysical uncertainties. This remarkable result holds not only for the scenario of gravitino dark matter with broken R -parity, but also for any other scenario of decaying dark matter with lifetime $\sim 10^{26} \text{ s}$ which decays predominantly into Z^0 and/or W^\pm gauge bosons with momentum $\sim 50 \text{ GeV}$.

Antiproton flux

The general antimatter transport equation can be simplified by taking into account that energy losses are negligible for antiprotons. Using this approximation, we have solved the diffusion equation for three propagation models consistent with the B/C ratio which yield the minimum (MIN), median (MED) and maximal (MAX) antiproton flux [30]. We have found that the Green’s function which describes antiproton propagation from dark matter decay can be approximated by the following in-

¹ The same conclusion has been independently reached by Ishiwata, Matsumoto and Moroi in [18].

TABLE 2. Coefficients of the interpolating function Eq. (8) for the antiproton Green’s function assuming a NFW halo profile and for the MIN, MED and MAX propagation models defined in [30].

model	x	y	z
MIN	-0.0537	0.7052	-0.1840
MED	1.8002	0.4099	-0.1343
MAX	3.3602	-0.1438	-0.0403

terpolating function [17]:

$$G_{\bar{p}}(T, T') \simeq 10^{14} e^{x+y \ln T + z \ln^2 T} \delta(T' - T) \text{cm}^{-3} \text{s}, \quad (8)$$

which, again, is valid for any decaying dark matter particle. The coefficients x , y and z for the NFW profile can be found in Table 2 for the different diffusion models. In this case the approximation is accurate to a 5-10%. As in the case of the positrons, the dependence of the Green’s function on the halo model is fairly weak.

The interstellar antiproton flux can be then straightforwardly computed from Eqs. (4) and Eq. (5) using the previous parametrization of the Green’s function and the energy spectrum of antiprotons from gravitino decay, $dN_{\bar{p}}/dT$. However, this is not the antiproton flux measured by balloon or satellite experiments, which is affected by solar modulation. In the force field approximation [34] the effect of solar modulation can be included by applying the following simple formula that relates the antiproton flux at the top of the Earth’s atmosphere and the interstellar antiproton flux [35]:

$$\Phi_{\bar{p}}^{\text{TOA}}(T_{\text{TOA}}) = \left(\frac{2m_p T_{\text{TOA}} + T_{\text{TOA}}^2}{2m_p T_{\text{IS}} + T_{\text{IS}}^2} \right) \Phi_{\bar{p}}^{\text{IS}}(T_{\text{IS}}), \quad (9)$$

where $T_{\text{IS}} = T_{\text{TOA}} + \phi_F$, with T_{IS} and T_{TOA} being the antiproton kinetic energies at the heliospheric boundary and at the top of the Earth’s atmosphere, respectively, and ϕ_F the solar modulation parameter, which we take $\phi_F = 500$ MV.

We show in Fig. 3 the predicted antiproton flux from gravitino decay for the MIN, MED and MAX diffusion models when $m_{3/2} \simeq 150$ GeV and $\tau_{3/2} \simeq 1.3 \times 10^{26}$ s. From the plot, the extreme sensitivity of the primary antiproton flux to the choice of the diffusion model is apparent: parameters that successfully reproduce the observed B/C ratio lead to antiproton fluxes that span over two orders of magnitude. For a wide range of propagation parameters, the total antiproton flux is well above the observations and thus our scenario is most likely excluded. However, the MIN model yields a primary flux that is below the measured flux and thus might be compatible with observations.

We have analyzed more carefully the predictions for the MIN model computing the different contributions to

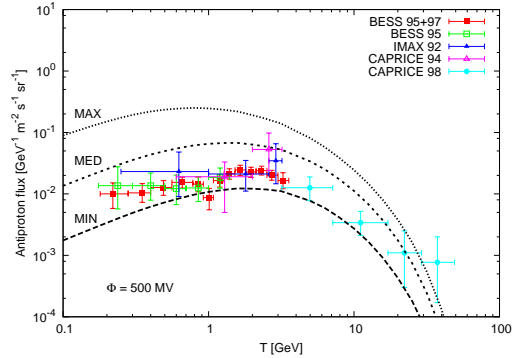


FIGURE 3. Contribution to the antiproton flux at the top of the atmosphere from the decay of dark matter gravitinos for the NFW halo profile and the MIN, MED and MAX propagation models. Gravitino parameters are as in Fig. 1.

the total antiproton flux. The result is shown in the right panel of Fig 4, where, for consistency, we have adopted as background the secondary antiproton flux calculated in [36] for the same MIN model. Although the primary antiproton flux is smaller than the measured one, the total antiproton flux is a factor of two above the observations. Nevertheless, in view of all the uncertainties that enter in the calculation of the antiproton flux, it might be premature to conclusively rule out the scenario of decaying gravitino dark matter. Namely, in addition to the uncertainties stemming from degeneracies in the diffusion parameters, there are also uncertainties from the nuclear cross sections and, to a lesser extent, uncertainties from the description of the interstellar medium and solar modulation (for a discussion of the various uncertainties see [36]). Furthermore, we used a simplified diffusion model that neglects the effects of reacceleration, energy losses and tertiary contributions. Therefore, there could be certain choices of parameters or more refined diffusion models where the total antiproton flux is consistent with experiments².

CONCLUSIONS

The scenario of gravitino dark matter with broken R -parity naturally reconciles three popular paradigms that seem to be in mutual conflict: supersymmetric dark matter, Big Bang Nucleosynthesis and thermal leptogenesis. Moreover, the gravitino decay products might become observable, thus opening the possibility of the indirect detection of the elusive gravitino dark matter.

² Some works have reported a deficit in the predicted secondary antiprotons compared to the observations and argued that this deficit could be connected with a contribution of primary antiprotons [37].

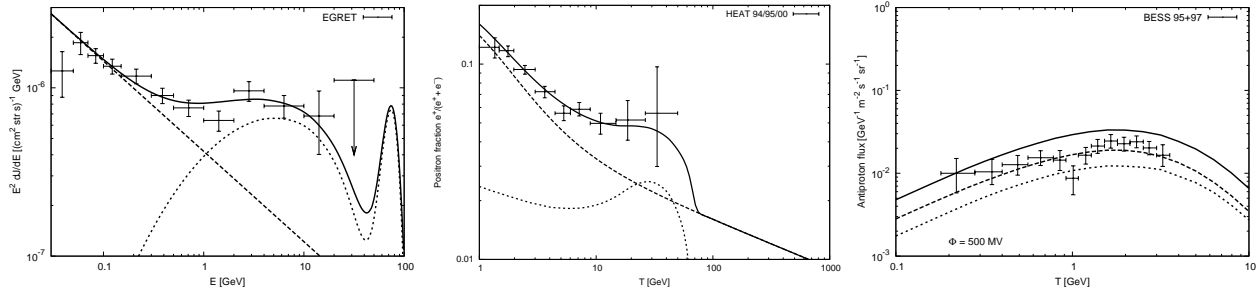


FIGURE 4. Summary of the signatures of gravitino dark matter decay in the extragalactic gamma-ray flux (left), the positron fraction (middle) and the antiproton flux (right), compared to the EGRET, HEAT and BESS data respectively. The contribution from gravitino decay is shown with a dotted line, the background with a dashed line and the total flux with a solid line. In these plots, we have adopted the MIN diffusion model, $m_{3/2} \simeq 150 \text{ GeV}$ and $\tau_{3/2} \simeq 1.3 \times 10^{26} \text{ s}$.

We have shown that the EGRET anomaly in the extragalactic gamma-ray flux and the HEAT excess in the positron fraction can be simultaneously explained by the decay of a gravitino with a mass $m_{3/2} \sim 150 \text{ GeV}$ and a lifetime of $\tau_{3/2} \sim 10^{26} \text{ s}$. However, the predicted antiproton flux tends to be too large, although the prediction suffers from large uncertainties and might be compatible with present observations for certain choices of propagation parameters. Our results are summarized in Fig. 4.

This remarkable result holds not only for the scenario of gravitino dark matter with broken R -parity, but also for any other scenario of decaying dark matter with lifetime $\sim 10^{26} \text{ s}$ which decays predominantly into Z^0 and/or W^\pm gauge bosons with momentum $\sim 50 \text{ GeV}$.

Acknowledgements I would like to thank my collaborators G. Bertone, W. Buchmüller, L. Covi, M. Grefe, K. Hamaguchi, T. T. Yanagida and especially D. Tran for a very pleasant and fruitful collaboration.

REFERENCES

1. G. Bertone, D. Hooper and J. Silk, Phys. Rept. **405** (2005) 279.
2. H. Pagels and J. R. Primack, Phys. Rev. Lett. **48** (1982) 223.
3. M. Bolz, A. Brandenburg and W. Buchmüller, Nucl. Phys. B **606** (2001) 518.
4. M. Fukugita and T. Yanagida, Phys. Lett. B **174** (1986) 45.
5. S. Davidson and A. Ibarra, Phys. Lett. B **535** (2002) 25; W. Buchmüller, P. Di Bari and M. Plümacher, Annals Phys. **315** (2005) 305.
6. D. N. Spergel *et al.* [WMAP Collaboration], Astrophys. J. Suppl. **170** (2007) 377.
7. M. Kawasaki, K. Kohri and T. Moroi, Phys. Rev. D **71** (2005) 083502.
8. M. Pospelov, Phys. Rev. Lett. **98** (2007) 231301.
9. K. Hamaguchi *et al.* Phys. Lett. B **650** (2007) 268.
10. T. Kanazaki *et al.* Phys. Rev. D **75** (2007) 025011.
11. J. L. Diaz-Cruz, J. R. Ellis, K. A. Olive and Y. Santoso, JHEP **0705** (2007) 003.
12. M. Ratz, K. Schmidt-Hoberg and M. W. Winkler, arXiv:0808.0829 [hep-ph]; J. Pradler and F. D. Steffen, arXiv:0808.2462 [hep-ph].
13. J. Pradler and F. D. Steffen, Phys. Lett. B **648** (2007) 224.
14. W. Buchmüller, L. Covi, K. Hamaguchi, A. Ibarra and T. Yanagida, JHEP **0703**, 037 (2007).
15. F. Takayama and M. Yamaguchi, Phys. Lett. B **485** (2000) 388.
16. A. Ibarra and D. Tran, Phys. Rev. Lett. **100** (2008) 061301.
17. A. Ibarra and D. Tran, JCAP **0807** (2008) 002.
18. K. Ishiwata, S. Matsumoto and T. Moroi, arXiv:0805.1133 [hep-ph].
19. T. Sjöstrand *et al.*, JHEP **0605** (2006) 026.
20. J. F. Navarro, C. S. Frenk and S. D. M. White, Astrophys. J. **462** (1996) 563.
21. L. Covi, M. Grefe, A. Ibarra and D. Tran. To appear.
22. A. W. Strong, I. V. Moskalenko and O. Reimer, Astrophys. J. **613** (2004) 962; Astrophys. J. **613** (2004) 956.
23. S. W. Barwick *et al.* [HEAT Collaboration], Astrophys. J. **482** (1997) L191.
24. S. Orito *et al.* [BESS Collaboration], Phys. Rev. Lett. **84** (2000) 1078; H. Matsunaga *et al.*, Phys. Rev. Lett. **81** (1998) 4052.
25. <http://fermi.gsfc.nasa.gov/>
26. P. Picozza *et al.*, Astropart. Phys. **27** (2007) 296. See also the Web page <http://pamela.roma2.infn.it/index.php>.
27. G. Bertone, W. Buchmüller, L. Covi and A. Ibarra, JCAP **0711** (2007) 003.
28. See for example V. S. Berezinskii, S. V. Buolnov, V. A. Dogiel, V. L. Ginzburg, V. S. Ptuskin, Astrophysics of Cosmic Rays (Amsterdam: North-Holland, 1990).
29. D. Maurin *et al.* Astrophys. J. **555** (2001) 585.
30. T. Delahaye *et al.* Phys. Rev. D **77** (2008) 063527.
31. E. A. Baltz and J. Edsjo, Phys. Rev. D **59** (1999) 023511.
32. E. A. Baltz, J. Edsjo, K. Freese and P. Gondolo, Phys. Rev. D **65**, 063511 (2002).
33. I. V. Moskalenko and A. W. Strong, Astrophys. J. **493** (1998) 694.
34. L. J. Gleeson and W. I. Axford, Astrophys. J. **149** (1967) L115; Astrophys. J. **154** (1968) 1011.
35. J. S. Perko, Astron. Astrophys. **184** (1987) 119.
36. F. Donato *et al.* Astrophys. J. **563** (2001) 172.
37. I. V. Moskalenko *et al.* Astrophys. J. **565** (2002) 280.